

Carrier recombination losses in inverted polymer: Fullerene solar cells with ZnO hole-blocking layer from transient photovoltage and impedance spectroscopy techniques

Pablo P. Boix,¹ Jon Ajuria,² Roberto Pacios,² and Germà Garcia-Belmonte^{1,a)}

¹Photovoltaic and Optoelectronic Devices Group, Departament de Física, Universitat Jaume I, ES-12071 Castelló, Spain

²Department of Microsystems, IKERLAN-IK4, S. Cooperative Goiru Kalea 9, Polo Innovación Garaia, ES-20500 Arrasate-Mondragón, Gipuzkoa, Spain

(Received 15 December 2010; accepted 4 February 2011; published online 11 April 2011)

In this study, full coincidence between impedance spectroscopy and transient photovoltage techniques in measuring recombination kinetics of photogenerated charge carriers in inverted polymer:fullerene organic solar cells with ZnO hole-blocking layer is reported. Carrier lifetime exhibits values at illumination intensities near 1 sun within the microseconds time scale. Photogenerated charge carrier density attains values within 10^{15} – 10^{16} cm⁻³. Decay kinetics is analyzed by means of a bimolecular recombination law with a recombination coefficient slightly dependent on the charge density, which lies within the order of $k \sim 10^{-12}$ cm³ s⁻¹. It is also demonstrated that inverted-processed cells exhibit capacitance, recombination resistance, and lifetime parameters comparable to those extracted from regular cells, despite the great differences between the contact structures of these kinds of devices.

© 2011 American Institute of Physics. [doi:10.1063/1.3561437]

I. INTRODUCTION

Conducting organic compounds are at the heart of bulk-heterojunction (BHJ) solar cells, formed by an interpenetrating blend of an optically active polymer and electron accepting molecules, and constitute a very promising route toward cheap and versatile solar cells. Particularly, the combination of poly(3-hexylthiophene) (P3HT) and [6,6]-phenyl C₆₁-butyric acid methyl ester (PCBM) in organic blends has shown high photovoltaic performance.¹ Solution-processed polythiophene:fullerene cells achieved between 6% and 8% power conversion efficiency using novel materials as well as the additives optimizing the phase separation.^{2,3} Despite recent improvements, efficiency is still below the limit established by theoretical studies.⁴

Carrier recombination corresponding to charge transfer events between electrons in the acceptor and holes in the donor after charge separation, also known as nongeminate recombination, is a particularly important loss mechanism in bulk-heterojunction organic solar cells. Because of the large internal interface appearing as a consequence of donor/acceptor blending, charge separation into different materials is favored after photogeneration. However, the interpenetrated morphology simultaneously enhances the carrier recombination through charge transfer between acceptor and donor molecules. Recombination mechanisms have two main detrimental consequences on the cell operation. (a) Short-circuit current might be reduced if the carriers recombine before reaching the outer interfaces. Its effect depends upon the recombination time value in comparison to the typical carrier transit times. Because high internal quantum efficiency is usu-

ally encountered in these organic photovoltaic systems, approaching even 100% values,⁵ it is derived that both geminate and nongeminate recombination influence on short-circuit current must be low in case of high efficiency devices. (b) The previous observation entails that energy conversion efficiency is mainly limited by the output photovoltage.⁴ Carrier recombination plays a determining role in establishing the achievable open-circuit voltage.⁵ Solar cells in steady-state, open-circuit conditions under continuous irradiation functions by the kinetic balance established between charge generation and recombination rates, $G = U$. In open-circuit conditions, no direct current is allowed ($j_{dc} = 0$) so as to strictly satisfy $j_{gen} = j_{rec}$. The photovoltaic system accumulates photogenerated electrons n at the acceptor levels and holes p at the donor levels, and their concentrations will be stated by the mentioned kinetic balance. In the simplest version $U = n/\tau$, which entails that $n = G\tau$, τ being the electron recombination time. Storage of charge carriers has the effect of enlarging the Fermi level splitting, which effectively determines the output open-circuit voltage as $-qV_{oc} = E_{Fn} - E_{Fp}$, q being the elementary charge. Hence, the output voltage measured in open-circuit conditions monitors the splitting of the Fermi levels, which in turn are stated by the charge carrier concentrations.⁵

Carrier recombination time (lifetime) is a parameter highly dependent upon the solar cell working conditions. Temperature and particularly electron and hole carrier concentrations, and their respective distributions within the existing density-of-states (DOS) should be considered in developing a microscopic model for recombination.⁵ As pointed out by Bisquert *et al.*, proper definition of the lifetime is only strictly feasible by considering a small perturbation of a given steady-state.⁶ If the electron recombination rate per unit volume is U_n , the decay of the population is governed by the general equation

^{a)}Author to whom correspondence should be addressed. Electronic mail: garsiag@fca.uji.es.

$$\frac{dn}{dt} = -U_n(n). \quad (1)$$

Assuming a perturbation of the existing carrier density much smaller than the average, steady-state concentration $\Delta n \ll \bar{n}$, the decay equation is

$$\frac{d\Delta n}{dt} = -\left(\frac{\partial U_n}{\partial n}\right)_{\bar{n}} \Delta n. \quad (2)$$

Small perturbation allows for the linearization of Eq. (1) which gives an exponential law (first-order decay) and permits defining a lifetime in terms of the recombination rate U_n as

$$\tau_n = \left(\frac{\partial U_n}{\partial n}\right)_{\bar{n}}^{-1}. \quad (3)$$

Equation (3) clearly establishes that lifetime is only well defined at a given steady-state, which has important implications in selecting an experimental technique for measuring the recombination kinetics. A well-sustained determination of the lifetime helps identifying proper microscopic recombination mechanisms. Several recombination-related issues have been recently addressed: origin of the reduced bimolecular recombination,⁷ effect of trapping,⁸ dependence of lifetime on photogenerated carrier density,⁹ or influence of disorder (DOS distributions).¹⁰ Progress in elucidating which aspects are relevant needs for an exact determination of lifetime under controlled experimental conditions.

Several techniques have been proposed to extract carrier recombination time in organic solar cells. A family of techniques combine pulsed illumination and applied bias changes to collect photogenerated charges and derive transport and recombination parameters. Among these techniques one can find photoinduced charge extraction in linearly increasing voltage (photo-CELIV),¹¹ integral mode time-of-flight,¹² and dark current injection.¹³ These methods use bias voltage sweeps much larger than 1 V and are characterized by the fact that photovoltaic devices do not operate under continuous irradiation. Since large biases are applied, current transient decays hardly exhibit exponential responses, and the derived lifetime (or recombination coefficient) results time-dependent. By using such techniques it is feasible to determine only an “effective” lifetime.¹¹ Although widely adopted, these large-amplitude techniques have limited application when a deeper knowledge on recombination mechanisms is aimed.

There exists another set of techniques that measure a transient response induced by a pulse of light which perturbs a steady-state. Transient absorption spectroscopy¹⁴ (TAS) is an optical measuring approach which monitors changes in optical density after photogeneration to extract the decay kinetics of excess carriers. A related method is based on modulated photoinduced absorption.¹⁵ Similarly, transient photovoltage⁹ (TPV) and photocurrent (TPC) allows for parameter extraction (lifetime and photoinduced carrier density) in conditions of continuous irradiation and small-amplitude perturbation. In addition to transient techniques, frequency-modulated methods also fulfill the condition of applying a small-amplitude perturbation on a given steady-state. Among these modulation methods, impedance spectroscopy

(IS) is a widely used tool which has provided enormous success for the determination of energetic and kinetic factors governing the operation of dye-sensitized solar cells (DSC) at voltages close to V_{oc} .¹⁶ Recently, IS has been also applied in the determination of lifetime and capacitances in organic BHJ devices.^{10,17} In the case of DSC, determination of electron lifetimes by IS has been validated with independent methods of measurement, such as open-circuit voltage decay.¹⁸ In inorganic solar cells, it is possible to apply contactless methods to determine minority carrier lifetime,¹⁹ and IS results are in agreement with these methods too.²⁰ Hence, convergence of different parameter extraction methods is a crucial test for elucidating the validity of the measuring approach. Noticeably, differences of 1 order of magnitude between recombination coefficient extracted from photo-CELIV and TPV techniques have been reported for organic photovoltaic solar cells.²¹ Such a discrepancy has been attributed to the great difference in device operation between small-amplitude perturbation of continuous irradiation (TPV) and short intense light pulse out of steady-state by applying a large voltage ramp (photo-CELIV).

We report in this paper the application of IS to determine recombination kinetics of BHJ solar cells in working conditions, in comparison to TPV experiments using inverted-type BHJ solar cells. Remarkably, we demonstrate that both techniques give coincident lifetime values which reinforce the validity of small-amplitude compared to large-amplitude techniques for measuring carrier lifetime in organic solar cells. We also point out that inverted-processed cells exhibit capacitance and parallel (recombination) resistance parameters comparable to those extracted from regular cells, despite the great differences between the contact structures of these kinds of devices. This is then an indication of the bulk-related, rather than outer interface-related, origin of the electrical parameters analyzed.

II. EXPERIMENTAL

Solar cells of structure ITO/ZnO/P3HT:PCBM/PEDOT:PSS/Au were built according to the following procedure: ITO coated glass substrates were cleaned by ultrasonic treatments in acetone and isopropyl alcohol. For devices containing ZnO as the hole-blocking layer, a nanoparticle dispersion was prepared according Pacholski method.²² Briefly, 0.11 g of zinc acetate dihydrate was dissolved in 50 ml of methanol under vigorous stirring at 60 °C. Subsequently, a 0.03 M solution of KOH (25 ml) was added dropwise in methanol at 60 °C. The reaction mixture was stirred for 2 h at 60 °C. The obtained colloidal suspension, without any further purification treatment, was spin casted at 2000 rpm during 30 s on the substrate. The thickness of the ZnO layer is estimated to be ~10 nm. The ZnO deposition process was followed by a 5 min air annealing at 150 °C.

The P3HT:PCBM solution was prepared by mixing 25:25 mg in 1 ml of chlorobenzene. The solution was then heated overnight at 80 °C. Dr. Blade was used to coat the P3HT:PCBM film: The plate temperature was set to 60 °C and the blade speed to 25 mm/s. The substrate was then covered for 90 s with a Petri dish for slow drying of the film.

These coating conditions resulted in a film thickness of 350 nm. PEDOT:PSS (AI 4083 from H.C. Stark) with the addition of 1% surfactant and heated to 90 °C was spin cast on top of the P3HT:PCBM film and annealed in a glovebox at 110 °C for 10 min, yielding thicknesses of around 50 nm. Device fabrication was completed by thermal evaporation of gold at room temperature under vacuum at a base pressure of 4×10^{-6} mbar. The deposited area of the electrode defines an active area of 9 mm².

TPV experiments were performed following a procedure previously reported⁹ by connecting the devices to a high input impedance oscilloscope (1 M Ω) which allows measuring V_{oc} under variation of a white light illumination. A nitrogen pumped-dye pulsed laser of 596 nm wavelength was used to generate a small perturbation on V_{oc} ($\Delta V_{oc} < 20$ mV). Because the system is in open-circuit conditions, V_{oc} decay is proportional to the photogenerated excess carriers relaxation ($d\Delta V_{oc}/dt \propto d\Delta n/dt$) that allows directly measuring the carrier lifetime. IS measurements were performed with an Autolab PGSTAT-30 equipped with a frequency analyzer module. AC oscillating amplitude was as low as 20 mV (rms) to maintain the linearity of the response. Measurements were performed at zero current conditions by applying a bias which equals V_{oc} at varying continuous irradiation conditions. The devices used in this study exhibited good rectifying behavior. Photovoltaic response was observed to result in conversion efficiencies around 3%.

III. RESULTS AND DISCUSSION

Experiments were performed using solar cells of inverted structure ITO (indium tin oxide)/ZnO/P3HT:PCBM/PEDOT:PSS [poly(3,4-ethylenedioxythiophene): poly(styrene sulfonic acid)]/Au always at room temperature. A representative example of typical TPV signals is shown in Fig. 1 for different illumination intensities. It is observed that decays exhibit an approximate straight line in log-linear scale that informs about the first-order character of the excess carrier relaxation law as expected for small-amplitude conditions [Eq. (2)]. Lifetime τ can be readily extracted from the slope since $\Delta V_{oc} \propto \exp(-t/\tau)$. Lifetime

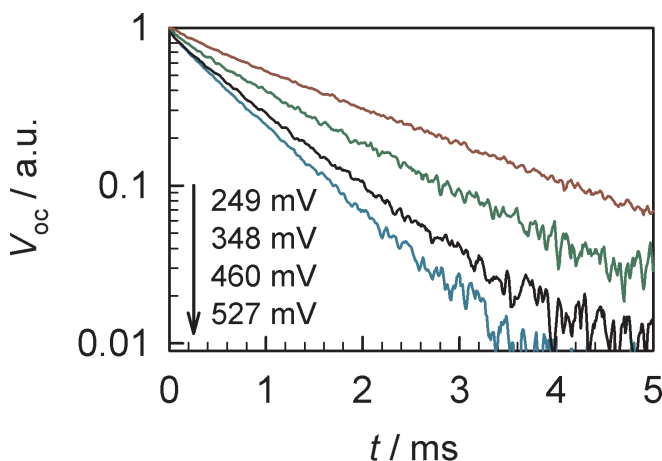


FIG. 1. (Color online) Normalized TPV signals produced by a small-amplitude laser pulse on inverted organic solar cells with ZnO hole-blocking layer. Different steady-state open-circuit values are indicated.

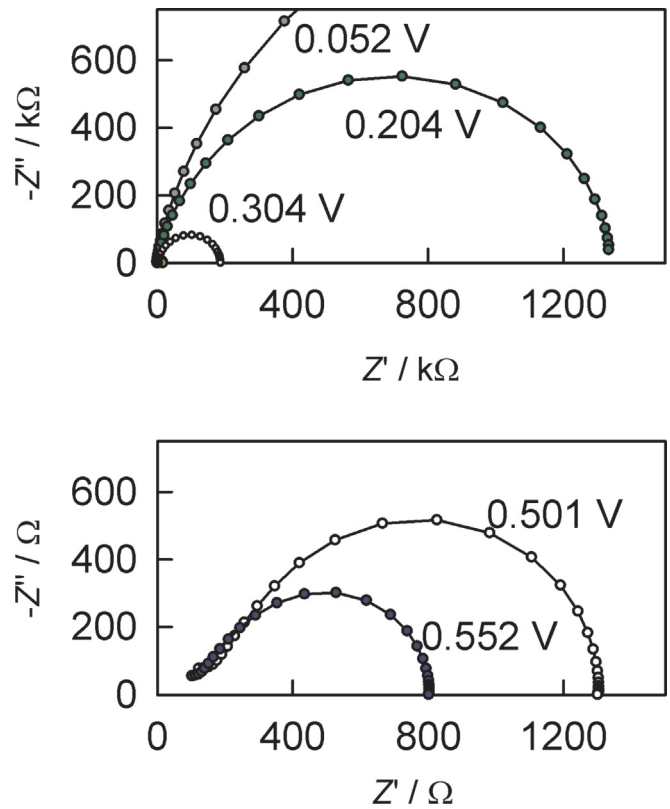


FIG. 2. (Color online) Example of impedance spectroscopy spectra registered in open-circuit conditions at different white light illumination intensities. Low-frequency arc is produced by the parallel connection of recombination resistance R_{rec} and charge storage, chemical capacitance C_{μ} . Carrier lifetime is calculated from $\tau = R_{rec}C_{\mu}$.

decreases as V_{oc} increases, indicating that the amount of charge carriers enhances electrical losses in agreement with a bimolecular recombination mechanism (Fig. 3). The impedance results at different illumination intensities are shown in Fig. 2. The applied bias voltage compensates the effect of the photovoltage so that the cell is effectively measured at open-circuit conditions, i.e., photocurrent is canceled by the recombination flow and $j_{dc} = 0$. The spectra are characterized by a major RC arc plus additional minor features at high frequency, as found in previous reports.¹⁰ The low-frequency arc is attributed to the processes of photogenerated carrier recombination (resistance R_{rec}) and storage (chemical capacitance C_{μ}) in the photoactive blend.⁶ Then, this main arc defines a time constant which is interpreted as the excess carrier lifetime, $\tau = R_{rec}C_{\mu}$. By examining Fig. 3, one can infer that both experimental techniques extract similar carrier lifetime values. Recombination mechanism depends on V_{oc} by following an approximate exponential behavior as $\tau \propto \exp(-\gamma V_{oc}/k_B T)$, being $k_B T$ the thermal energy and $\gamma \approx 0.39$. These results found for inverted cells are in good agreement with previous analysis performed on regular deposition devices.^{10,17}

A deeper analysis of the recombination mechanism is based on a bimolecular law for the relaxation of photogenerated charge carriers as²³

$$\frac{dn}{dt} = -k(n)n^2, \quad (4)$$

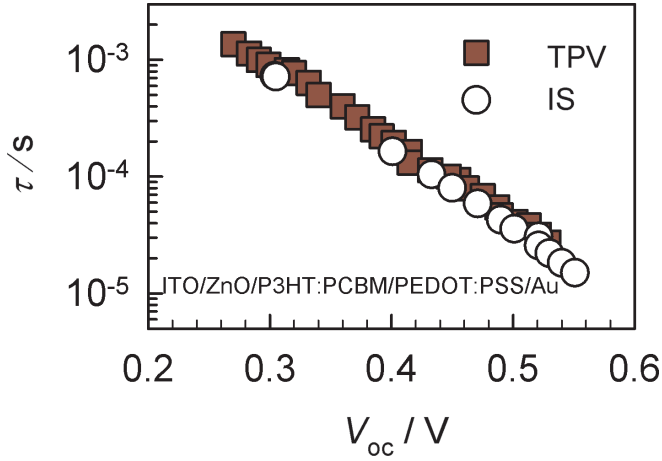


FIG. 3. (Color online) Comparison of carrier lifetime extracted from TPV and IS techniques on inverted organic solar cells with ZnO hole-blocking layer.

where $k(n)$ represents a carrier density-dependent recombination coefficient. Additionally, electroneutrality $n = p$ is assumed. For a small perturbation of carriers, either produced by the laser pulse (TPV) or ac applied voltage (IS) $\Delta n \ll n$, Eq. (4) results in

$$\frac{d\Delta n}{dt} = -2k(n)n\Delta n - \frac{\partial k(n)}{\partial n}n^2\Delta n, \quad (5)$$

which allows straightforwardly defining the carrier lifetime since the second summand has a minor weight. By following Eq. (2), one obtain

$$\tau = \frac{1}{2k(n)n}. \quad (6)$$

It is shown in Fig. 4(a), chemical capacitance and recombination resistance parameters extracted from IS. As pointed out in previous publications,¹⁰ from the capacitance dependence on V_{oc} , it is feasible to estimate the charger carrier density by integration of $C_{\mu}(V_{oc})$ curve, which is in fact a representation of the carrier DOS as $C_{\mu} = q^2g(V_{oc})$. We suggested¹⁰ that the recombination losses restrict the electronic site occupancy to the tail of the DOS because surviving photogenerated carriers thermalize into deeper lying states. Gaussian¹⁰ as well as exponential⁹ DOS have been proposed accounting for the electron states distribution, although it is hard distinguishing between both in practical experiments because usual illumination intensities are able to reach only low-occupancy conditions (10^{14} – 10^{17} cm^{-3}). Interestingly, the case of full occupation of intermediate electronic bands has been recently reported.¹⁷ Dependences of both resistance and capacitance on V_{oc} exhibit exponential laws as $C_{\mu} \propto \exp(\alpha V_{oc}/k_B T)$ and $R_{rec} \propto \exp(-\beta V_{oc}/k_B T)$ with $\alpha = 0.26$ and $\beta = 0.65$, respectively. Figure 4(b) allows observing that $\tau \propto n^{-\delta}$, with $1 \leq \delta < 2$. Values of $\delta = 1$ have been reported signaling a constant, carrier density-independent recombination coefficient k .¹⁰ More commonly $\delta > 1$ (Ref. 9) which has been interpreted in terms of a trapping-mediated recombination mechanism.⁸ Nevertheless the

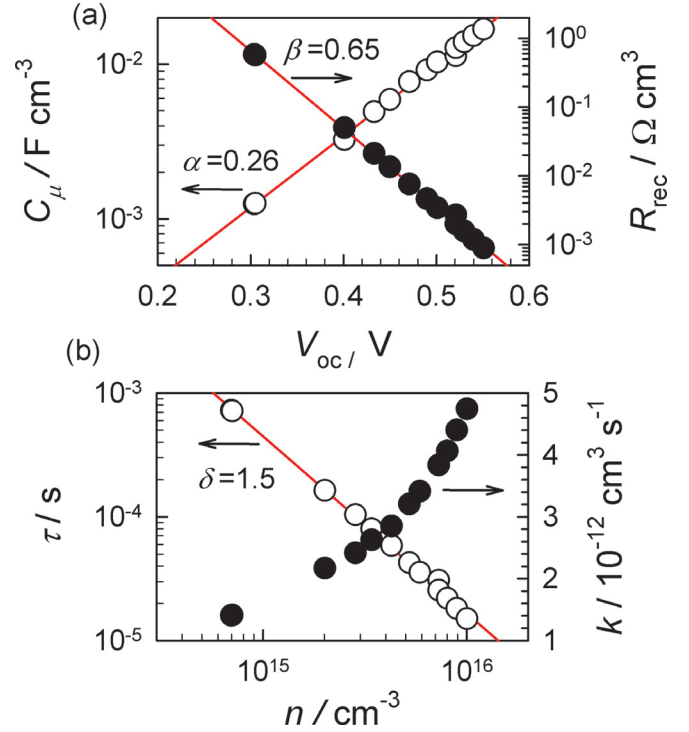


FIG. 4. (Color online) (a) Recombination resistance and chemical capacitance extracted from IS. Both parameters exhibit an exponential dependence on V_{oc} as $C_{\mu} \propto \exp(\alpha V_{oc}/k_B T)$, and $R_{rec} \propto \exp(-\beta V_{oc}/k_B T)$ with $\alpha = 0.26$, and $\beta = 0.65$, respectively. If an exponential tail of trapping states is assumed as $g(E) \propto \exp(E/k_B T_0)$, then $\alpha = T/T_0$ being T_0 the characteristic temperature of the exponential distribution. (b) Carrier lifetime as a function of the photogenerated carrier density, exhibiting a power-law as $\tau \propto n^{-\delta}$ with $\delta = 1.5$. Recombination coefficient k calculated using Eq. (6).

enhancement in the recombination kinetics at photogenerated carrier density within 10^{15} – 10^{16} cm^{-3} lies within the same order of magnitude of $k \sim 10^{-12}$ $\text{cm}^3 \text{s}^{-1}$ [Fig. 4(b)], in good agreement with previous reports on recombination kinetics in BHJ P3HT:PCBM-based solar cells.^{10,21,24}

It is worth noticing that the impedance method allows establishing a direct relation between the exponents of the capacitance and resistance dependences on V_{oc} , and the power-law exponent of the $\tau(n)$ function as

$$\delta = \frac{\beta}{\alpha} - 1. \quad (7)$$

From the previous discussion, one can infer that the rate of recombination is proportional to the $(1 + \delta)$ th order of carrier concentration as $dn/dt \propto n^{1+\delta} \propto n^{\beta/\alpha}$, which depends not only on the features of the DOS [accessible from the capacitance variation on V_{oc} and represented by $\alpha = T/T_0$, T_0 being the characteristic temperature of the exponential distribution $g(E) \propto \exp(E/k_B T_0)$], but also on the flux of carrier loss through the parameter β . Some recent studies have linked the order of the relaxation law exclusively to the energy distribution of the trapped states as $\delta = 1/\alpha$.^{25,26} These analyses see the recombination as a multiple trapping mechanism in which trapped holes can either recombine with electrons at the acceptor levels or be retrapped at an exponential tail of donor states. However, our experimental observation in Eq. (7) entails that the information provided

solely by the energy distribution of tail (trapping) states is not enough to derive the correct order of the relaxation law.²⁷ It is reasonable that the microscopic recombination coefficient depends on the relative energy distance between acceptor and donor levels participating in the recombination event and not being energy-independent. An energy-dependent k would entail that the measured recombination resistance, related to the recombination flux as $R_{\text{rec}} \propto (dj_{\text{rec}}/dV_{\text{oc}})^{-1}$, should be taken into account in deriving microscopic recombination models.

Finally, we want to emphasize that a proper interpretation of the carrier lifetime in BHJ solar devices should rely upon separating the influence of carrier density and energetic location (by measuring chemical capacitance and described by α for an exponential DOS), from the effect of the recombination flux (through the analysis of the recombination resistance represented by β parameter).

IV. CONCLUSIONS

We report on the application of IS to determine recombination kinetics of BHJ solar cells in working conditions, in comparison to TPV experiments using inverted-type BHJ solar cells. We observe that both techniques give coincident lifetime values what reinforces the validity of small-amplitude in front of large-amplitude techniques for measuring the carrier lifetime in organic solar cells. Lifetime at illumination intensities of 1 sun exhibits values around 10 μs , while photo-generated charge carrier density attains values within order of 10^{16} cm^{-3} . We also demonstrate that inverted-processed cells are characterized by chemical capacitance, recombination resistance, and lifetime parameters comparable to those extracted from regular cells, despite the great differences between the contact structures of these kinds of devices. This is then a strong indication of the bulk-related, rather than outer interface-related, origin of the electrical parameters analyzed. Impedance spectroscopy measurements should then be a useful starting point to properly derive meaningful and consistent device BHJ models.

ACKNOWLEDGMENTS

We acknowledge the financial support from Ministerio de Educacion y Ciencia under project HOPE CSD2007-00007

(Consolider-Ingenio 2010), Generalitat Valenciana (PROMETEO/2009/058) and Universitat Jaume I (P1.1B2008-32).

- ¹W. Ma, C. Yang, X. Gong, K.-S. Lee, and A. J. Heeger, *Adv. Funct. Mater.* **15**, 1617 (2005).
- ²J. Peet, J. Y. Kim, N. E. Coates, W. L. Ma, D. Moses, A. J. Heeger, and G. C. Bazan, *Nature Mater.* **6**, 497 (2007).
- ³S. H. Park, A. Roy, S. Beaupré, S. Cho, N. Coates, J. S. Moon, D. Moses, M. Leclerc, K. Lee, and A. J. Heeger, *Nat. Photonics* **3**, 297 (2009).
- ⁴T. Kirchartz, K. Taretto, and U. Rau, *J. Phys. Chem. C* **113**, 17958 (2009).
- ⁵G. Garcia-Belmonte and J. Bisquert, *Appl. Phys. Lett.* **96**, 113301 (2010).
- ⁶J. Bisquert, F. Fabregat-Santiago, I. Mora-Seró, G. Garcia-Belmonte, and S. Giménez, *J. Phys. Chem. C* **113**, 17278 (2009).
- ⁷C. Deibel, A. Wagenpahl, and V. Dyakonov, *Phys. Rev. B* **80**, 075203 (2009).
- ⁸T. M. Clarke, F. C. Jamieson, and J. R. Durrant, *J. Phys. Chem. C* **113**, 20934 (2009).
- ⁹C. G. Shuttle, B. O'Regan, A. M. Ballantyne, J. Nelson, D. D. C. Bradley, J. de Mello, and J. R. Durrant, *Appl. Phys. Lett.* **92**, 093311 (2008).
- ¹⁰G. Garcia-Belmonte, P. P. Boix, J. Bisquert, M. Sessolo, and H. J. Bolink, *Sol. Energy Mater. Sol. Cells* **94**, 366 (2010).
- ¹¹A. J. Mozer, G. Dennler, N. S. Sariciftci, M. Westerling, A. Pivrikas, R. Österbacka, and G. Juska, *Phys. Rev. B* **72**, 035217 (2005).
- ¹²A. Pivrikas, G. Juska, A. J. Mozer, M. Scharber, K. Arlauskas, N. S. Sariciftci, H. Stubb, and R. Österbacka, *Phys. Rev. Lett.* **94**, 176806 (2005).
- ¹³G. Juska, G. Sliuzys, K. Genevicius, K. Arlauskas, A. Pivrikas, M. Scharber, G. Dennler, N. S. Sariciftci, and R. Österbacka, *Phys. Rev. B* **74**, 115314 (2006).
- ¹⁴I. Montanari, A. F. Nogueira, J. Nelson, J. R. Durrant, C. Winder, M. A. Loi, N. S. Sariciftci, and C. Brabec, *Appl. Phys. Lett.* **81**, 3001 (2002).
- ¹⁵C. Arndt, U. Zhokhavets, M. Mohr, G. Gobsch, M. Al-Ibrahim, and S. Sensfuss, *Synth. Met.* **147**, 257 (2004).
- ¹⁶Q. Wang, S. Ito, M. Grätzel, F. Fabregat-Santiago, I. Mora-Seró, J. Bisquert, T. Bosshoa, and H. Imaic, *J. Phys. Chem. B* **110**, 19406 (2006).
- ¹⁷G. Garcia-Belmonte, P. P. Boix, J. Bisquert, M. Lenes, H. J. Bolink, A. La Rosa, S. Filippone, and N. Martín, *J. Phys. Chem. Lett.* **1**, 2566 (2010).
- ¹⁸A. Zaban, M. Greenshtein, and J. Bisquert, *ChemPhysChem* **4**, 859 (2003).
- ¹⁹R. A. Sinton and A. Cuevas, *Appl. Phys. Lett.* **69**, 2510 (1996).
- ²⁰I. Mora-Seró, Y. Luo, G. Garcia-Belmonte, J. Bisquert, D. Muñoz, C. Voz, J. Puigdollers, and R. Alcubilla, *Sol. Energy Mater. Sol. Cells* **92**, 505 (2008).
- ²¹A. Foertig, A. Baumann, D. Rauh, V. Dyakonov, and C. Deibel, *Appl. Phys. Lett.* **95**, 052104 (2009).
- ²²C. Pacholski, A. Kornowski, and H. Weller, *Angew. Chem., Int. Ed. Engl.* **41**, 1188 (2002).
- ²³C. G. Shuttle, B. O'Regan, A. M. Ballantyne, J. Nelson, D. D. C. Bradley, and J. R. Durrant, *Phys. Rev. B* **78**, 113201 (2008).
- ²⁴R. Hamilton, C. G. Shuttle, B. O'Regan, T. Hammant, J. Nelson, and J. R. Durrant, *J. Phys. Chem. Lett.* **1**, 1432 (2010).
- ²⁵M. Tachiya and K. Seki, *Phys. Rev. B* **82**, 085201 (2010).
- ²⁶M. P. Eng, P. A. Barnes, and J. R. Durrant, *J. Phys. Chem. Lett.* **1**, 3096 (2010).
- ²⁷J. Bisquert and I. Mora-Seró, *J. Phys. Chem. Lett.* **1**, 450 (2010).